*Desalination and Water Treatment*
www.deswater.com
doi: 10.5004/dwt.2021.27580

241 (2021) 310–317
November

# Collapse mechanism and protection of buried pipelines in frozen soil area under hydro-thermal-mechanical coupling analysis

Yang Zhang[a,b], Jingtai Niu[a], Jingmin Liu[c,*]

[a]*School of Water Conservancy and Ecological Engineering, Nanchang Institute of Technology, Nanchang 330099, China*
[b]*China Institute of Water Resources and Hydropower Research, Beijing 100038, China*
[c]*School of Civil Engineering and Architecture, Guangxi University of Science and Technology, Liuzhou 545006, China, email: liujingmin1990@163.com*

Received 29 June 2021; Accepted 23 September 2021

**ABSTRACT**

The collapse mechanism of buried pipelines in frozen soil areas is explored to protect buried pipelines. The classical hydrodynamic model and the basic theory of thermoelasticity are used to construct a hydro-thermal-mechanical coupling mathematical model suitable for frozen soil. It can be divided into two steps: the full coupling of water and heat and the one-way coupling of water, heat and force. The geometric model is established and the network is divided. The analyzed hydro-thermal results are imported into the model. The frost heave deformation of the buried pipeline surface in the frozen soil area is simulated and analyzed. The collapse mechanism of buried pipelines in frozen soil areas is combined and studied. The vertical stress of the buried pipeline increases with the increase of the relative stiffness of the pipe soil. The research shows that the larger the diameter of the buried pipeline is in the frozen soil area, the easier it is to collapse and the greater the displacement of the buried pipeline is. Moreover, the vertical stress on the pipeline increases with the increase of the pipe diameter.

*Keywords:* Coupling of water and heat; Frozen soil area; Buried pipeline; Pipeline collapse

## 1. Introduction

Frozen soil is an anisotropic, heterogeneous four-item complex composed of gas, water, ice, and soil particles. The components of frozen soil influence and restrict each other. The freezing process is the result of the interaction of various factors such as water, heat and force [1]. Soil particles, ice and unfrozen water in frozen soil affect each other under the action of external conditions such as temperature. Its movement, diffusion and phase change lead to freeze-thaw changes in the soil. The law of water and heat changes in soil and the redistribution of stress are the main factors that cause frost heave and thaw settlement. Frost heave and thaw settlement are the most common diseases that affect the collapse of buried pipelines in frozen soil engineering [2]. Therefore, to ensure the stability of buried pipelines in permafrost regions, the temperature field and stress status of the foundation under the coupling effects of water, heat and force need to be observed.

In the process of freezing and thawing, the frost heave of soil is affected by the coupling of moisture field, temperature field and stress field. The problem of soil frost heave is an extremely complex and comprehensive problem. If only a single factor is studied, it is difficult to reveal the true process of frost heave. The influence of the coupling effect of multi-physics (water, heat, force) on the frost heave problem should be comprehensively considered [3]. The hydro-thermal coupling analysis is the basis of the

* Corresponding author.

hydro-thermal-mechanical coupling analysis. Based on the hydro-thermal-mechanical coupling analysis, the collapse mechanism and protection of buried pipelines in frozen soil areas are studied and analyzed. The collapse mechanism and protection of buried pipelines in frozen soil areas are conducive to perfecting the theory of frost heave, further understanding the frost heaving process, and improving the collapse of buried pipelines in frozen soil areas.

Based on the classic hydrodynamic model and the basic theory of thermoelasticity, a mathematical model of hydro-thermal-mechanical coupling suitable for frozen soil is constructed. It can be divided into two steps: the full coupling of water and heat and the one-way coupling of water, heat and force. The frost heave deformation of the buried pipeline surface in the frozen soil area is simulated and analyzed. The collapse mechanism of buried pipelines in frozen soil areas is obtained. Protective measures for buried pipelines in frozen soil areas are further proposed.

## 2. Method

### *2.1. Ideas for constructing hydro-thermal-mechanical coupling model*

To avoid using the controversial Claberon equation to describe the influence of temperature on soil water potential, the model built is based on a hydrodynamic model. Mainly focusing on the macro perspective, the freezing law of the soil is analyzed. The non-condensation criterion and the initiation mechanism of ice lens are studied microscopically [4]. In terms of coupling equations, based on the coupling relationship between the temperature field and the moisture field, a hydro-thermal fully coupled model is constructed. Based on the analysis results of the temperature field and the moisture field, the knowledge of thermodynamics is used to realize the one-way coupling of water, heat and force. Finally, the hydro-thermal-mechanical coupling frost heave model is proposed.

Firstly, starting from the basic principles of conservation of mass and energy, Darcy's law, Fourier's law, soil–water characteristic curve, and solid–liquid ratio are introduced. The hydro-thermal fully coupled model is derived. The hydro-thermal coupling model is used as the basis. Considering the similarity between soil freezing and frost heaving and thermal expansion of general materials, the linear expansion coefficient is introduced. The stress-strain balance equation is constructed [5]. Through the hydrothermal model and the stress-strain balance equation, the one-way coupling of the soil moisture field, temperature field and displacement field is realized.

### *2.2. Basic equations of hydro-thermal-mechanical coupling model*

The hydro-thermal-mechanical coupling model is realized in two steps. The first step is the full coupling of water and heat. The basic equations are: water control equation, temperature control equation and connection equation. The second step is the one-way coupling of hydrothermal and force, and the basic equation is the stress-strain governing equation [6].

#### *2.2.1. Equation of moisture control*

For general soil, when water migrates in saturated or unsaturated soil, there is only seepage and no phase change. There are negative temperature zones in positive frozen soil. In the process of water migration, ice-water phase change will occur. Experimental studies show that the frost heave caused by the phase transition of the migration water is much greater than the frost heave deformation caused by the in-situ water. It is the main reason for the frost heave [7]. For unsaturated frozen soil, the water migration model is the key to study the change of the water field inside the soil. Temperature potential and matrix potential are the driving force for water migration. The model is based on the principle of conservation of mass and Darcy's law, and the water control equation is constructed.

Darcy passed the saturated sand permeability test and found that the seepage flow is proportional to the difference between the upstream and downstream heads and the cross-sectional area perpendicular to the direction of the water flow. The seepage volume is inversely proportional to the seepage length. According to this, Darcy's law is summed up.

$$q = KI \tag{1}$$

where $q$ is the water flux (m s$^{-1}$). $I$ is the hydraulic gradient. $K$ is the permeability coefficient, also known as the moisture conductivity and hydraulic conductivity (m s$^{-1}$).

$$I = \frac{\Delta H}{L} \tag{2}$$

where $\Delta H$ is the total head difference between the beginning and the end of the permeation path (m). $L$ is the linear length of the penetration path (m).

It is worth noting that Eq. (2) is for the constant flow of homogeneous soil. The water head changes nonlinearly along with the flow. In heterogeneous soil or unsteady flow, it is more reasonable to express Darcy's law in differential form.

$$q = -K\frac{dH}{dL} \tag{3}$$

Since the permeability coefficient $K$ in Eq. (3) is a constant related to soil quality, this equation is only applicable to saturated soil. $K$ in unsaturated soil will change with the change of water content. Therefore, the constant $K$ can be rewritten as a variable $K(\theta)$ related to the volumetric water content. Then Darcy's law is extended to unsaturated soil, and its spatial expression is as follows.

$$q = -K(\theta_u)\left(\frac{d\psi}{dx} + \frac{d\psi}{dy} + \frac{d\psi}{dz}\right) = -K(\theta_u)\text{grad}\psi = -K(\theta_u)\nabla\psi \tag{4}$$

where $\theta_u$ is the volume of unfrozen water content, and $\psi$ is the soil water potential (m). $\nabla$ or grad is the gradient operator.

#### 2.2.2. Temperature control equation

The biggest difference between the heat transfer process of frozen soil and the general heat transfer process under positive temperature is the existence of ice–water phase transition. There will be latent heat generated in the micro-element body. The heat generated by the ice–water phase change is defined as the heat source in the micro-element body [8]. According to the law of conservation of energy, the increase $Q$ of the thermal energy of the micro-element soil is equal to the sum of the net heat transfer heat of the micro-element body $Q_1$, the increase of the mass transfer heat $Q_2$, and the heat generation $Q_3$ of the heat source.

$$Q = Q_1 + Q_2 + Q_3 \tag{5}$$

When some researchers use the principle of conservation of mass, to simplify the model, the increase in mass transfer heat $Q_2$ is small, which is often considered negligible. At present, the simplified treatment of this heat has not been sufficiently verified by experiments, especially for the different soil qualities of buried pipelines in frozen soil areas [9]. Therefore, when constructing the temperature control equation, this term should be taken into account in the differential equation.

In the increment $dt$ at any time, the increased $Q$ of the thermal energy of the micro-element soil is as follows.

$$Q = C\frac{\partial T}{\partial t}dxdydzdt \tag{6}$$

where $C$ is the volumetric heat capacity (kJ m$^{-3}$ K$^{-1}$). $C$ is related to the content of each component of the soil. $T$ is the temperature (K), and $t$ is time (s).

In the increment $dt$ at any time, the net heat transfer amount $Q_1$ of the micro-element body can be expressed as follows.

$$Q_1 = Q_{1x} + Q_{1y} + Q_{1z} \tag{7}$$

where subscripts $x$, $y$, and $z$ respectively represent the components along the corresponding coordinate axis.

The net heat transfer component along the $x$-axis is as follows.

$$Q_{1x} = J_{\mathrm{Tx}}dydzdt - \left(J_{\mathrm{Tx}} + \frac{\partial J_{\mathrm{Tx}}}{\partial x}\mathrm{d}x\right)dydzdt = -\frac{\partial J_{\mathrm{Tx}}}{\partial x}dxdydzdt \tag{8}$$

where $J_{\mathrm{Tx}}$ is the component of the heat flux JT (W m$^{-2}$) in the $x$-direction.

In the same way, the net heat transfer components in the $y$ and $z$ directions can be obtained.

$$Q_{1y} = J_{\mathrm{Ty}}dxdzdt - \left(J_{\mathrm{Ty}} + \frac{\partial J_{\mathrm{Ty}}}{\partial y}dy\right)dxdzdt = -\frac{\partial J_{\mathrm{Ty}}}{\partial y}dxdydzdt \tag{9}$$

$$Q_{1z} = J_{\mathrm{Tz}}dxdydt - \left(J_{\mathrm{Tz}} + \frac{\partial J_{\mathrm{Tz}}}{\partial z}dz\right)dxdydt = -\frac{\partial J_{\mathrm{Tz}}}{\partial z}dxdydzdt \tag{10}$$

where $J_{\mathrm{Ty}}$ and $J_{\mathrm{Tz}}$ are the components of the heat flux JT (W m$^{-2}$) in the $y$ and $z$ directions.

Heat transfer in porous media is known from Fourier's law.

$$J_T = -\lambda\nabla T \tag{11}$$

$$J_T = J_{\mathrm{Tx}} + J_{\mathrm{Ty}} + J_{\mathrm{Tz}} \tag{12}$$

$$J_{\mathrm{Tx}} = \frac{\partial J_T}{\partial x}`J_{\mathrm{Ty}} = \frac{\partial J_T}{\partial y}`J_{\mathrm{Tz}} = \frac{\partial J_T}{\partial z} \tag{13}$$

where $\lambda$ is the thermal conductivity (W m$^{-1}$ K$^{-1}$). $\lambda$ is related to the content of each component of the soil.

Combining Eqs. (8)–(13) can obtain the net heat transfer heat $Q_1$ of the micro-element body in the space coordinate system.

$$Q_1 = -\nabla\cdot\left(-\lambda\nabla T\right)dxdydzdt \tag{14}$$

Within the increment $dt$ at any time, the mass transfer heat increase $Q_2$ in the micro-element body is the heat carried by the migrating water.

$$Q_2 = -C_W q\nabla T dxdydzdt \tag{15}$$

where CW is the volumetric heat capacity (kJ m$^{-3}$ K$^{-1}$). $q$ is the flux (permeation flow rate) (m s$^{-1}$), and $T$ is the temperature (K).

Within the increment $dt$ at any time, the calorific value $Q_3$ in the micro-element body is as follows.

$$Q_3 = L\rho_i\frac{\partial\theta_i}{\partial t}dxdydzdt \tag{16}$$

where $L$ is the latent heat of phase change (kJ/kg).

Eqs. (4), (7), (14)–(16) are substituted into Eq. (5), and the temperature control differential equation is obtained.

$$C\frac{\partial T}{\partial t} + C_W\left[-K\left(\theta_u\right)\nabla\left(\varphi_p^m + z\right)\right]\nabla T + \nabla\left(-\lambda\nabla T\right) - L\rho_i\frac{\partial\theta_i}{\partial t} = 0 \tag{17}$$

#### 2.2.3. Contact equation

One of the basic hydraulic properties of unsaturated soils is the change of matrix potential with volumetric water content. The relationship between matrix potential and volumetric water content is often described by the soil–water characteristic curve (SWCC) [10]. On the basis of SWCC, the specific water capacity (differential water capacity) Cm (m–1) is commonly used to characterize the relationship between matrix potential and volumetric water content.

$$C_m = \frac{\partial\theta_u}{\partial\varphi_p^m} \tag{18}$$

In unsaturated soil, the soil moisture diffusion coefficient $D$ (m$^2$ s$^{-1}$) can be expressed as follows.

$$D = \frac{K}{C_m} = \frac{K}{\frac{\partial\theta_u}{\partial\varphi_p^m}} = K\frac{\partial\varphi_p^m}{\partial\theta_u} \tag{19}$$

The matrix potential term in Eq. (17) can be expressed as follows.

$$K(\theta_u)\nabla(\varphi_p^m + z) = K(\theta_u)\frac{\partial\varphi_p^m}{\partial\theta_u}\nabla\theta_u + K(\theta_u)\nabla z = D\nabla\theta_u + K(\theta_u) \tag{20}$$

During the freezing process, liquid water can not completely phase into ice. There is always a certain amount of liquid water around the soil particles. There is a dynamic equilibrium relationship between the volume of unfrozen water (liquid water) and temperature in frozen soil, which is usually characterized by SFC soil freezing characteristics. Generally speaking, there is a positive correlation between unfrozen water content and temperature [11]. The main factors affecting the content of unfrozen water are soil quality, external conditions (temperature, load) and freeze-thaw history. To explore the influence of different influencing factors on the unfrozen water content of frozen soil, scholars in China and other countries have conducted a large number of experimental studies on this from different angles. The unfrozen water prediction model proposed by Xu is referred to [21].

$$\frac{w_o}{w_u} = \left(\frac{T}{T_f}\right)^b \tag{21}$$

where $w_o$ is the initial mass water content, $w_u$ is the quality of unfrozen water content, $T$ is the soil temperature (°C), $b$ is the empirical constant, and $T_f$ is the freezing temperature (°C).

There is a conversion relationship of Eq. (22) between the mass unfrozen water content and the volume unfrozen water content $\theta_u$.

$$w_u = \frac{m_u}{m_s} = \frac{\rho_w v_u}{m_s} = \frac{\frac{\rho_w v_u}{v}}{\frac{m_s}{v}} = \frac{\frac{\rho_w v_u}{v}}{\rho_d} = \frac{\rho_w}{\rho_d}\theta_u \tag{22}$$

where $m_u$ is the mass of unfrozen water (kg), $m_s$ is the mass of soil skeleton (kg), $v_u$ is the volume of unfrozen water (m$^3$), $v$ is the total volume of the soil (m$^3$). $\varrho_d$ is the dry density of soil (kg m$^{-3}$).

To characterize the dynamic balance relationship of a $\theta_u - T$ and $\theta_u - \theta_1$ at the same time, now Eq. (18) is transformed as follows.

$$\frac{w_o}{w_u} = \frac{w_i + w_u}{w_u} = \frac{\rho_i\theta_i + \rho_w\theta_u}{\rho_w\theta_u} = \frac{\rho_i}{\rho_w}\frac{\theta_i}{\theta_u} + 1 = \left(\frac{T}{T_f}\right)^b \tag{23}$$

In summary, the basic governing Eqs. (4) and (17) and the related Eqs. (20) and (23) are combined. The moisture field and temperature field of the soil at any time are solved. The established mathematical model can directly view the volumetric unfrozen water content, volumetric ice content and the mass water content corresponding to the sum in the solution results. There is no need to invert the volume of unfrozen water content or solve the volumetric ice content twice, which makes the solution process simple and easy.

#### 2.3.4. Stress—strain control equation

The soil is assumed to be an isotropic linear elastic material. The influence of the self-weight of the soil and the expansion of the ice-water phase change on the deformation is considered. According to the basic theory of elastic mechanics, the relationship between soil stress and physical strength satisfies the equilibrium differential equation of Eq. (24).

$$\begin{cases} \frac{\partial\sigma_x}{\partial x} + \frac{\partial\tau_{yx}}{\partial y} + \frac{\partial\tau_{zx}}{\partial z} + f_x = 0 \\ \frac{\partial\sigma_y}{\partial y} + \frac{\partial\tau_{zy}}{\partial z} + \frac{\partial\tau_{xy}}{\partial x} + f_y = 0 \\ \frac{\partial\sigma_z}{\partial z} + \frac{\partial\tau_{xz}}{\partial x} + \frac{\partial\tau_{yz}}{\partial y} + f_z = 0 \end{cases} \tag{24}$$

To simplify writing, the above formula can be expressed as follows.

$$\nabla \bullet [\sigma] + [F_V] = 0 \tag{25}$$

where $\nabla\bullet$ is the differential operator (divergence div). $[F_V]$ is the physical strength matrix. $[\sigma]$ is the stress matrix.

The $[F_V]$ and $[\sigma]$ scores of the same-sex spatial bodies are as follows.

$$[F_V] = \begin{bmatrix} f_x & f_y & f_z \end{bmatrix}^T \tag{26}$$

$$[\sigma] = \begin{bmatrix} \sigma_x & \sigma_y & \sigma_z & \tau_{xy} & \tau_{xz} & \tau_{yz} \end{bmatrix}^T \tag{27}$$

where $f$ is the volume force (N m$^{-3}$), $\sigma$ is the normal stress (N m$^{-2}$), $\tau$ is the shear stress (N m$^{-2}$). The subscripts $x$, $y$, $z$ are the corresponding directions of the $x$, $y$, and $z$ coordinate axes weight.

To simplify the model, the influence of the self-weight of the soil and the expansion of the ice–water phase change on the deformation is mainly considered. Only $[\varepsilon_{th}]$ is considered in the inelastic strain term. The simplified equation is as follows.

$$\nabla \bullet \left[[D]\left([\varepsilon] - [\varepsilon_{th}]\right)\right] + [F_V] = 0 \tag{28}$$

Eq. (28) is the differential equation of frozen soil stress–strain control. The coefficient of linear expansion is generally a function of temperature $T$. To fully consider the comprehensive effect of moisture field and temperature field on deformation, the mass ice content is adopted to express

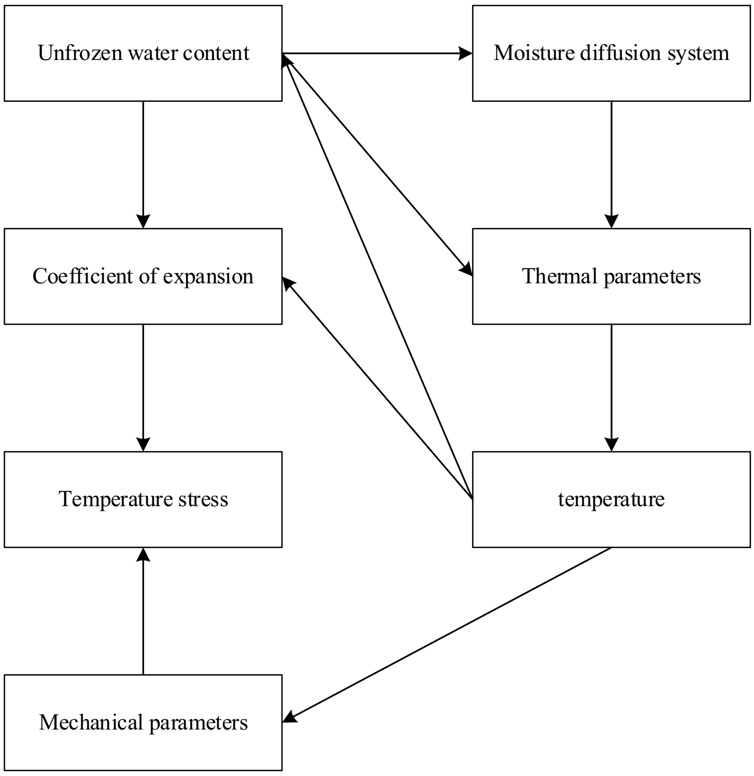


Fig. 1. The mutual influence of water, heat and force.

the linear expansion coefficient. General researchers treat both elastic modulus and Poisson's ratio as fixed values. This type of treatment method does not take into account the influence of the freezing state of the soil on the mechanical parameters of the soil. However, this kind of parameter will change during the freezing process of the soil [12]. To make the model more reasonable, both the elastic modulus and Poisson's ratio are taken as functions of temperature, rather than constants.

The three factors of water, heat and force in frozen soil area can be related to temperature through unfrozen water content. The figure shows that when one of the factors changes, the other two factors change accordingly (Fig. 1). These three factors restrict each other on the basis of mutual influence, and jointly control the soil stability of buried pipelines in permafrost regions.

### 2.3. Classification of buried pipelines

Pipelines are classified according to pressure and medium temperature (Tables 1 and 2). When the pipeline conveys the medium under pressure, the pipeline must meet certain strength and tightness. When the main body of the pipeline and its connectors are subjected to medium pressure, the pipeline will not be damaged or leaked.

Buried pipelines can also be classified according to different pipe materials as shown in Fig. 2. According to different materials, there are mainly the following types.

According to actual investigations, the buried pipelines in China are mainly concrete and reinforced concrete pipelines. However, due to the characteristics and limitations of concrete materials, the existing concrete pipes are different [13]. However, PVC, PE and other materials are gradually replacing concrete pipes and reinforced concrete pipes due to the good corrosion resistance, flexibility and relatively lightweight.

Table 1
Classified by pressure pipeline

| Category name | Design pressure $P$ (MPa) |
|---|---|
| Vacuum pipeline | $P < 0$ |
| Low pressure pipeline | $0 < P \leq 1.6$ |
| Medium pressure pipeline | $1.6 < P \leq 10.0$ |
| High pressure pipeline | $10.0 < P \leq 42.0$ |

## 3. Results and discussion

### 3.1. Process of numerical simulation

The deformation caused by a frost heave is mainly considered. The soil is always in the positive temperature zone within a certain depth range. Under the condition of not affecting the deformation field analysis, to simplify the model, the position 11 m below the natural ground is regarded as the lower boundary of the model. The lower boundary has almost no displacement and is set as a fixed end [14]. The left and right boundary positions are set as

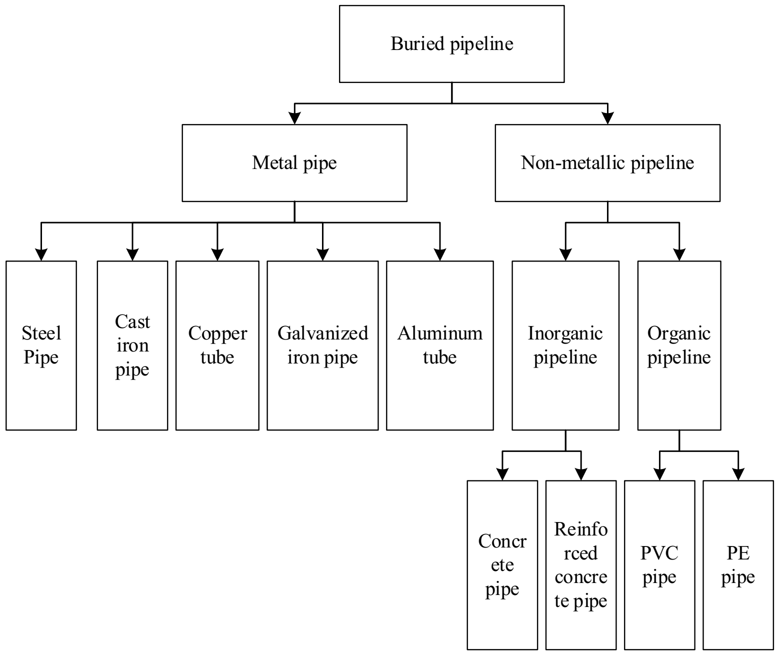


Fig. 2. Classified by pipe material.

roller support. There is no lateral displacement of the left and right boundary positions, only frost heave deformation occurs.

Firstly, the geometric model is established and the mesh is divided. The grid division density is the same as the setting in Chapter 3. Secondly, the previously analyzed hydrothermal results are imported into the model in the form of interpolation functions. In the solid mechanics interface, a linear elastic material model is used. The thermal expansion interface is introduced and related parameters are set. The input type of thermal expansion attribute adopts the secant coefficient of thermal expansion. The thermal expansion coefficients of the *A* and *B* groups of fillers and graded crushed stone layers are input using if judgment sentence and a minus sign are added. The thermal expansion coefficient of the clay loess layer is taken as a constant –0.0015. The strain reference temperature of each layer of soil is set as the freezing temperature. The temperature function $T$ is set to if ($T_t < T_f$, $T_f + \Delta T_c$, $T_f$) ($T_t$ is the soil temperature at the time of calculation. $\Delta T_c$ is the phase change interval and $T_f$ is the freezing temperature). The temperature function $T$ is used to determine whether the soil is in the phase change zone and whether it participates in the phase change frost heave calculation. Finally, the study type is set to a steady-state, and model calculations are performed.

The frost heave deformation of buried pipelines is distributed asymmetrically along the horizontal direction (Fig. 3). There is uneven deformation on the surface of the buried pipeline. The order of frost heave deformation on the surface of buried pipelines is the right side of the pipeline, the left side of the pipeline, and the centre of the pipeline. The frost heave deformation is the largest on the right, followed by the left, and the smallest at the centre of the pipe. The maximum frost heave deformation of the buried pipeline surface is about 11–18 mm. The part of the frost heave deformation exceeds the 15 mm required by the specification. The frost heave deformation of the soil is distributed asymmetrically along the transverse direction, and there is uneven deformation on the surface. There is no insulation layer on the left and right sides directly exposed to the surrounding environment. The track plate at the centre of the pipeline can be regarded as an insulation material that has the effect of slowing down temperature transfer. Therefore, in the negative temperature zone of the soil, uneven deformation occurred on the left and right sides and the centre of the pipeline in the early stage. The uneven deformation gradually increases with time (up to 14 mm), and after reaching a certain degree of freezing (February 15), the difference begins to gradually decrease. The uneven deformation in the centre of the pipeline is relatively small, and the maximum is not more than 2 mm.

### 3.2. Mechanism of pipeline collapse

The shear surface has friction on the soil on both sides of the pipe circumference. The fill on both sides of the pipe circumference create a downward friction on the shear surface. This frictional force acts on the backfilled soil column at the upper part of the pipeline. The vertical pressure of the buried pipeline is greater than the weight of the soil pillar of the backfill. According to the force balance equation, the vertical earth pressure on the pipe can be calculated. During the operation of the flexible pipeline, it is loaded by the earth pressure of the backfill on the upper part of the pipeline. The force of the flexible pipeline is related to the physical and mechanical properties of the pipeline material (such as the stiffness of the pipeline and bending deformation ability). The force of the flexible pipeline is also related to the characteristics of the backfill soil on the upper part of

Table 2
Classified by medium temperature pipeline

| Category name | Medium temperature $T$ (°C) |
|---|---|
| Cryogenic pipeline | $T < –40$ |
| Room temperature pipeline | $–40 < T \leq 120$ |
| Medium temperature pipeline | $120 < T \leq 450$ |
| High temperature pipeline | $450 < T$ |

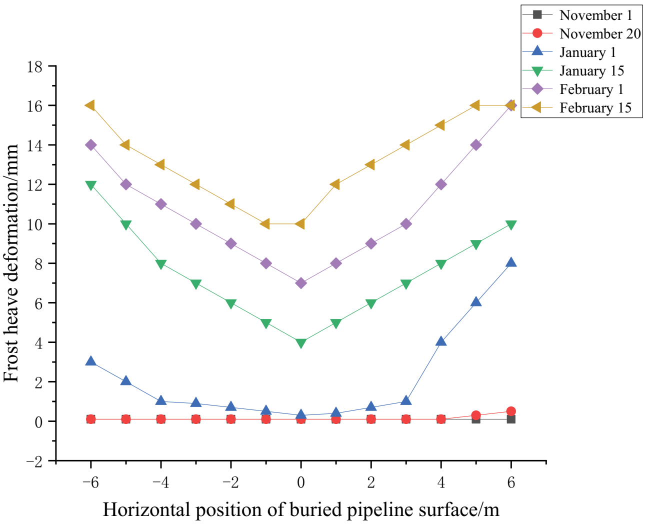


Fig. 3. Frost heave deformation of the pipe surface at different times.

the pipeline (load thickness, the friction coefficient between the backfill soil and the groove, the bulk density of the backfill soil, and the coefficient of internal friction of the backfill soil) [15].

The finite element simulation analysis results of the pipes with the same diameter and different quality show that the vertical stress of the pipe increases with the increase of the relative stiffness of the pipe soil. The results of finite element simulation analysis of force and deformation of pipes with the same quality and different diameters show that the larger the pipe diameter, the easier the pipe collapses and the greater the collapse displacement. The vertical stress on the pipeline increases with the increase of the pipe diameter. The finite element simulation analysis results of the pipe stress and deformation show that the maximum collapse displacement of the cast iron pipe occurs outside 1/5 of the pipe. The maximum collapse displacement of the remaining pipelines all occurred at about 1/3 of the pipeline [16–19].

### *3.3. Protective measures for buried pipelines*

The pipeline must be prevented before it is laid. The actual pipeline operation and construction conditions are investigated and the finite element analysis of the pipeline force is simulated. The following measures are obtained.

- Choosing the right pipe material is the most important and basic measure. The prevention of pipeline collapse mainly depends on the mechanical properties of the pipeline itself to resist the stress and strain experienced by the pipeline. Choosing the right pipe material can greatly reduce the probability of pipe collapse.
- The appropriate pipe diameter is selected. The larger the diameter of the pipe, the easier it is to collapse. Therefore, in the case of meeting the requirements of pipeline use, the pipeline with a small diameter is used as much as possible.
- Construction technology: The selection of scientific and reasonable construction technology when laying pipelines is also a major factor affecting pipeline collapse. Scientific and reasonable construction technology will also reduce the probability of pipeline collapse. For example, firstly, a layer of sand is used to compact the bottom of the pipe. Secondly, the pipeline is laid, and a layer of sand is spread on the top of the pipeline. Finally, the pipeline is covered with soil.
- The construction quality is controlled. The quality of construction will affect the collapse of the pipeline [20–22].

## 4. Conclusion

Based on the law of conservation of mass, law of conservation of energy, Darcy's law, Fourier's law and the basic theory of thermoelasticity, a mathematical model of hydro-thermal-mechanical coupling suitable for frozen soil is derived. The collapse mechanism of buried pipelines in frozen soil areas is studied. The finite element simulation analysis results of the force and deformation of pipelines with the same diameter and different quality show that the vertical stress of the buried pipeline increases with the increase of the relative stiffness of the pipe soil. The finite element simulation analysis results of the stress and deformation of buried pipelines of the same quality and different diameters show that the larger the diameter of the buried pipeline, the easier it is for the buried pipeline to collapse and the greater the collapse displacement. The vertical stress on the pipeline increases with the increase of the pipe diameter. Protective measures for buried pipelines in frozen soil areas are proposed to prevent the collapse of buried pipelines.

The macroscopic modeling idea of the classic hydrodynamic model is analogized. Based on the improved hydrodynamic model and related parameters, the basic theory of thermoelasticity is comprehensively considered. The solid-liquid ratio, soil-water characteristic curve (unsaturated soil unique), linear expansion coefficient and other related equations are used to realize the analysis of the hydro-thermal-mechanical coupling effect. However, the influence of vapor-phase water migration and vapor-liquid phase transition on hydro-thermal-mechanical coupling still needs to be considered. The water-heat-force-air coupling frost heave model is constructed. Under the actual roadway, the load on the pipeline is very complicated. The pipe force load needs to be considered more comprehensively.

## Acknowledgments

This study was supported by the science and technology project funded by the department of education of Jiangxi province (GJJ180951) and the National Natural Science Foundation of China (51969018).

## References


[1] F. Guo, H. Shi, M. Cheng, W. Gao, H. Yang, Q. Miao, A study of the insulation mechanism and anti-frost heave effects of polystyrene boards in seasonal frozen soil, Water, 10 (2018) 979, doi: 10.3390/w10080979.

[2] B. Dadfar, M.H. El Naggar, M. Nastev, Vulnerability of buried energy pipelines subject to earthquake-triggered transverse landslides in permafrost thawing slopes, J. Pipeline Syst. Eng. Pract., 9 (2018) 04018015, doi: 10.1061/(ASCE) PS.1949-1204.0000334.

[3] J.G. Lu, M.Y. Zhang, X.Y. Zhang, W.S. Pei, Review of the coupled hydro-thermo-mechanical interaction of frozen soil, J. Glaciol. Geocryology, 39 (2017) 102–111.

[4] H.W. Ran, J.H. Fan, J. Huang, Review of the coupling of water and heat in the freeze-thaw process and its model of frozen soil, Pratacultural Sci., 36 (2019) 991–999.

[5] S. Nasreen, M.A. Ashraf, Inadequate supply of water in agriculture sector of Pakistan due to depleting water reservoirs and redundant irrigation system, Water Conserv. Manage., 4 (2021) 13–19.

[6] H. Amin, B.A. Arain, T.M. Jahangir, A.R. Abbasi, J. Mangi, M.S. Abbasi, F. Amin, Copper (Cu) tolerance and accumulation potential in four native plant species: a comparative study for effective phytoextraction technique, Geol. Ecol. Landscapes, 5 (2021) 53–64.

[7] A.D. Tolche, Groundwater potential mapping using geospatial techniques: a case study of Dhungeta-Ramis sub-basin, Ethiopia, Geol. Ecol. Landscapes, 5 (2021) 65–80.

[8] T.V. Nwosu, E.C. Nnabuihe, M.J. Okafor, C.O. Madueke, Assessment of some physical properties of soil along an erosion prone watershed, Owerri-Imo State Nigeria, J. Clean WAS, 5 (2021) 10–16.

[9] S. Fatima, N. Aslam, S. Khalid, Effects of copper toxicity on different growth attributes of Phlox Drummondii, Environ. Ecosyst. Sci., 5 (2021) 58–63.

[10] S. Malik, Effect of climate change and its implications onward/toward Pakistan, Environ. Contamin. Rev., 3 (202) 13–15.

[11] M. Paudel, S. Regmi, A review on host preference, damage severity and integrated pest management of Red Pumpkin Beetle, Environ. Contamin. Rev., 3 (2020) 16–20.

[12] S.Y. Li, F.J. Niu, Z.Z. Sun, L.H. Shi, Numerical study on moisture-heat-mechanics coupled process of Jiangluling Tunnel construction in permafrost region, J. Glaciol. Geocryology, 40 (2018) 966–973.

[13] M. He, X.P. Feng, N. Li, Development of the extended finite element program for the thermo-hydro-mechanical coupling model of quasi-saturated freezing soil, Chin. J. Rock Mech. Eng., 36 (2017) 2798–2809.

[14] M. He, X.P. Feng, N. Li, et al., Improvement of coupled thermo-hydro-mechanical model for saturated freezing soil, Chin. J. Geotech. Eng., 40 (2018) 1212–1220.

[15] T. Wang, G. Zhou, L. Yin, L. Zhou, Estimation on the influence of seepage on stochastic thermal regime of frozen ground surrounding the crude oil pipeline, Cold Reg. Sci. Technol., 157 (2019) 13–20.

[16] J. Zhang, Y. Chen, B.F. Liang, B. Pan, Damage evolution mechanism of buried pipeline crossing reverse fault, J. Mech. Sci. Technol., 35 (2021) 71–77.

[17] H. Wang, Y. Yu, J. Yu, C. Jin, Y. Zhao, Z. Fan, Y. Zhang, Effect of 3D random pitting defects on the collapse pressure of pipe — Part II: numerical analysis, Thin-Walled Struct., 129 (2018) 527–541.

[18] H. Fang, P. Tan, X. Du, B. Li, K. Yang, Y. Zhang, Mechanical response of buried HDPE double-wall corrugated pipe under traffic-sewage coupling load, Tunnelling Underground Space Technol., 108 (2021) 103664, doi: 10.1016/j.tust.2020.103664.

[19] J. Zhang, J. Xie, Mechanical behaviour analysis of buried pipeline subject to ground loading, Pipeline Sci. Technol., 2 (2018) 303–309.

[20] D.Y. Wang, H. Zhu, Experimental study on buried pipeline instrumented with fiber optic sensors underground collapse, Chin. J. Geotech. Eng., 42 (2020) 1125–1131.

[21] L.W. Xu, X. Liu, F.Q. Chen, Mechanical analysis of buried suspended pipeline under the action of collapse, Eng. Mech., 35 (2018) 212–219, 228.

[22] W.P. Guo, Emergency measures for oil and gas transmission pipeline passing through mining subsidence area, Zhongzhou Coal, 40 (2018) 70–73,77.